IL NUOVO CIMENTO **47 C** (2024) 21
DOI 10.1393/ncc/i2024-24021-4

Colloquia: COMEX7

Rotational moments of inertia as indicators of the density dependence of the pairing functionals

Kenichi Yoshida(*)
Research Center for Nuclear Physics, Osaka University - Ibaraki, Osaka 567-0047 Japan

received 31 October 2023

Summary. — It is known that the moment of inertia (MoI) for the collective rotation is strongly influenced by the pairing correlation. The ground-state MoI is investigated for about 1700 even-even nuclei from the proton drip line to the neutron drip line up to $Z = 120$ and $N = 184$ to discuss the pairing properties in exotic nuclei. To this end, the cranked Skyrme-Hartree-Fock-Bogoliubov equation is solved in the coordinate space. This model describes well the available experimental data of more than 300 nuclides possessing an appreciable deformation. I find that the predicted MoI near the drip line depend on the choice of the pairing functional having different density dependence. A systematic measurement of the excitation energy and the transition probability to the first $I^\pi = 2^+$ state in neutron-rich nuclei can constrain the density dependence of the pairing functional.

1. – Introduction

Pairing and the emergence of superfluidity are universal collective behaviors occurring in many-fermionic systems. Superfluidity, typically defined as the ability of a liquid to flow through narrow channels without apparent friction, represents just one facet of its fascinating array of properties. Among these intriguing characteristics is the Hess-Fairbank effect [1], an extraordinary phenomenon observed when a liquid in a rotating container, cooled to the superfluid phase, transitions from initially rotating with the container to seemingly coming to rest. The moment of inertia (MoI) thus behaves non-classically.

The pairing correlation is a fundamental aspect of atomic nuclei, playing a crucial role in describing various static and spectroscopic properties. These properties include the energy gap observed in spectra of even-even nuclei, the phenomenon of odd-even staggering in binding energies, the strong collectivity exhibited in low-frequency quadrupole vibration, and the reduced MoI for rotation compared to rigid-body estimations [2, 3].

(*) E-mail: kyoshida@rcnp.osaka-u.ac.jp

Recently, various spectroscopic studies have been carried out to explore unique structures in neutron-rich nuclei. The excitation energy of the 2_1^+ state, $E(2_1^+)$, is often among the first quantities accessible in experiments and systematic measurements have revealed the evolution of the shell structure [4-6]. Besides the change of the shell structure associated with the onset of deformation, the $E(2_1^+)$ value may provide rich information on exotic nuclei. A significant lowering of the $E(2_1^+)$ value observed in the near-drip-line nucleus ^{40}Mg could be a signal of new physics in drip-line nuclei [7], as the theoretical calculations have predicted that the magnitude of deformation is not enhanced in ^{40}Mg comparing with the Mg isotopes with less neutrons [8-15]. The $E(2_1^+)$ value should be scrutinized by taking not only the deformation but the superfluidity into account.

Another critical issue in exploring the drip-line nuclei is a need for the careful treatment of the asymptotic part of the nucleonic density. An appropriate framework is Hartree-Fock-Bogoliubov (HFB) theory, solved in the coordinate-space representation [16]. This method has been used extensively in the description of spherical systems but is much more difficult to implement for systems with deformed equilibrium shapes. Therefore, calculations have been mostly restricted to axially symmetric nuclei [17-22]. A standard technique to describe the non-axial shapes is to employ a truncated single-particle basis, which consists of localized states and discretized-continuum oscillating states, for solutions of the HFB equation [23]. Such a method should not be able to describe adequately the spatial profile of densities at large distances. Recently, the HFB equation has been solved by employing the contour integral technique and the shifted Krylov subspace method for the Green's function [24, 25] to circumvent the successive diagonalization of the matrix with huge dimensions.

In the present paper, I investigate the rotational motion in neutron-rich nuclei, including drip-line nuclei, with an emphasis on pairing. Here, I study the lowest spin state, the 2_1^+ state, in even-even nonspherical nuclei. The MoI is evaluated microscopically by the self-consistent cranked-HFB employing the Skyrme-type energy-density functional (EDF) augmented with the pairing EDF. The calculated MoI is sensitive to the pairing EDF employed.

2. – Model

To describe the rotating superfluid nuclei, I directly solve the coordinate-space cranked Skyrme-HFB equation in the quasiparticle basis:

$$\sum_{\sigma'} \begin{bmatrix} h^{q\prime}_{\sigma\sigma'}(\boldsymbol{r}) & \tilde{h}^{q}_{\sigma\sigma'}(\boldsymbol{r}) \\ 4\sigma\sigma' \tilde{h}^{q*}_{-\sigma-\sigma'}(\boldsymbol{r}) & -4\sigma\sigma' h^{q\prime *}_{-\sigma-\sigma'}(\boldsymbol{r}) \end{bmatrix} \begin{bmatrix} \varphi^q_{1,\alpha}(\boldsymbol{r}\sigma') \\ \varphi^q_{2,\alpha}(\boldsymbol{r}\sigma') \end{bmatrix} = E_\alpha \begin{bmatrix} \varphi^q_{1,\alpha}(\boldsymbol{r}\sigma) \\ \varphi^q_{2,\alpha}(\boldsymbol{r}\sigma) \end{bmatrix}, \tag{1}$$

which is obtained by extending the formalism developed for describing the ground-state properties of even-even nuclei near the drip line [16]. Here the single-particle Routhian and the pair Hamiltonian are defined by using a Skyrme EDF combined with a pairing functional $E[\rho, \tilde{\rho}, \tilde{\rho}^*]$ as $h^{q\prime}_{\sigma\sigma'}(\boldsymbol{r}) = \frac{\delta E[\rho,\tilde{\rho},\tilde{\rho}^*]}{\delta \rho^q_{\sigma'\sigma}(\boldsymbol{r})} - (\lambda^q + \omega_{\rm rot} j_z)\delta_{\sigma\sigma'}$ and $\tilde{h}^q_{\sigma\sigma'}(\boldsymbol{r}) = \frac{\delta E[\rho,\tilde{\rho},\tilde{\rho}^*]}{\delta \tilde{\rho}^{q*}_{\sigma'\sigma}(\boldsymbol{r})}$. I define the z-axis as a quantization axis of the intrinsic spin and consider the system rotating uniformly about the z-axis with the rotational frequency $\omega_{\rm rot}$. The MoI is evaluated microscopically by the Thouless-Valatin procedure or equivalently the self-consistent cranking model as $\mathcal{J} = \lim_{\omega_{\rm rot}\to 0} \frac{J_z}{\omega_{\rm rot}}$ with $J_z = \langle \hat{J}_z \rangle$. I take the natural units: $\hbar = c = 1$.

I solve the CHFB equation by diagonalizing the HFB Hamiltonian in the three-dimensional (3D) Cartesian-mesh representation with the box boundary condition. Thanks to the reflection symmetries, I have only to consider the octant region explicitly in space with $x \geq 0$, $y \geq 0$, and $z \geq 0$; see refs. [26, 27] for details. I use a 3D lattice mesh $x_i = ih - h/2, y_j = jh - h/2, z_k = kh - h/2$ $(i, j, k = 1, 2, \cdots M)$ with a mesh size $h = 1.0$ fm and $M = 12$ for each direction. A reasonable convergence with respect to the mesh size h and the box size M is obtained for not only drip-line nuclei but medium-mass nuclei [28]. For diagonalizing the HFB matrix, I use the ScaLAPACK PDSYEV subroutine [29]. A modified Broyden's method [30] is utilized to calculate new densities during the self-consistent iteration. The quasiparticle energy is cut off at 60 MeV.

3. – Results and discussion

3˙1. *Validity of the model.* – The MoI of the ground state is evaluated at $\omega_{\rm rot} = 0.01$ MeV [31]. I employed the SkM* [32] and SLy4 [33] functionals augmented by the Yamagami-Shimizu-Nakatsukasa (YSN) pairing EDF [34], which is given as

$$\mathcal{E}_{\rm pair}(\boldsymbol{r}) = \frac{V_0}{4} \sum_{\tau={\rm n,p}} g_\tau[\rho, \rho_1] |\tilde{\rho}_\tau(\boldsymbol{r})|^2 \tag{2}$$

with

$$g_\tau[\rho, \rho_1] = 1 - \eta_0 \frac{\rho(\boldsymbol{r})}{\rho_0} - \eta_1 \frac{\tau_3 \rho_1(\boldsymbol{r})}{\rho_0} - \eta_2 \left[\frac{\rho_1(\boldsymbol{r})}{\rho_0}\right]^2. \tag{3}$$

Here, $\rho(\boldsymbol{r})$ and $\rho_1(\boldsymbol{r})$ are the isoscalar and isovector densities, $\tau =$ n (neutron) or p (proton), and $\rho_0 = 0.16$ fm^{-3} is the saturation density of symmetric nuclear matter. The parameters $V_0, \eta_0, \eta_1, \eta_2$ were optimized to reproduce the experimental pairing gaps globally and are summarised in table III of ref. [34]. Note that the parameters for the ρ_1 dependence η_1, η_2 are positive, and $\tau_3 = \pm 1$ for neutron/proton is introduced in the linear term of ρ_1 to preserve the charge symmetry of the pairing EDF. The YSN pairing functional was constructed based on the finding that the inclusion of the isospin dependence in the pairing functional gives a good reproduction of the pairing gaps in both stable and neutron-rich nuclei and in both symmetric nuclear matter and neutron matter [35, 36].

There are 657 even-even nuclei with known $E(2_1^+)$ [37]. In the present study, I limit the scope by excluding the very light nuclei ($Z < 10$), for which mean-field theory is least justified. This eliminates 22 nuclei. The experimental data evaluated as $3/E(2_1^+)$ for 635 nuclei are displayed in fig. 1(e). There is no collective rotation in spherical nuclei where the MoI is zero. Actually, I defined the spherical nuclei if the calculated MoI is less than 0.1 MeV^{-1}. Additional 273 (260) nuclei have been eliminated for that reason, leaving 362 (375) nuclei in the present analysis using the SkM* (SLy4) functional.

Figures 2(a) and 2(b) show the calculated MoI obtained by using SkM* and SLy4 *versus* experimental ones. The points follow the diagonal line reasonably well with some scatters that vary in extent over the different regimes. For transitional nuclei, one may wonder about the validity of the present model. The filled symbols in figs. 2(a) and 2(b) denote the weakly deformed nuclei with quadrupole deformation $\beta < 0.1$. These nuclei give a small value for the MoI, corresponding to higher $E(2_1^+)$ than measurement.

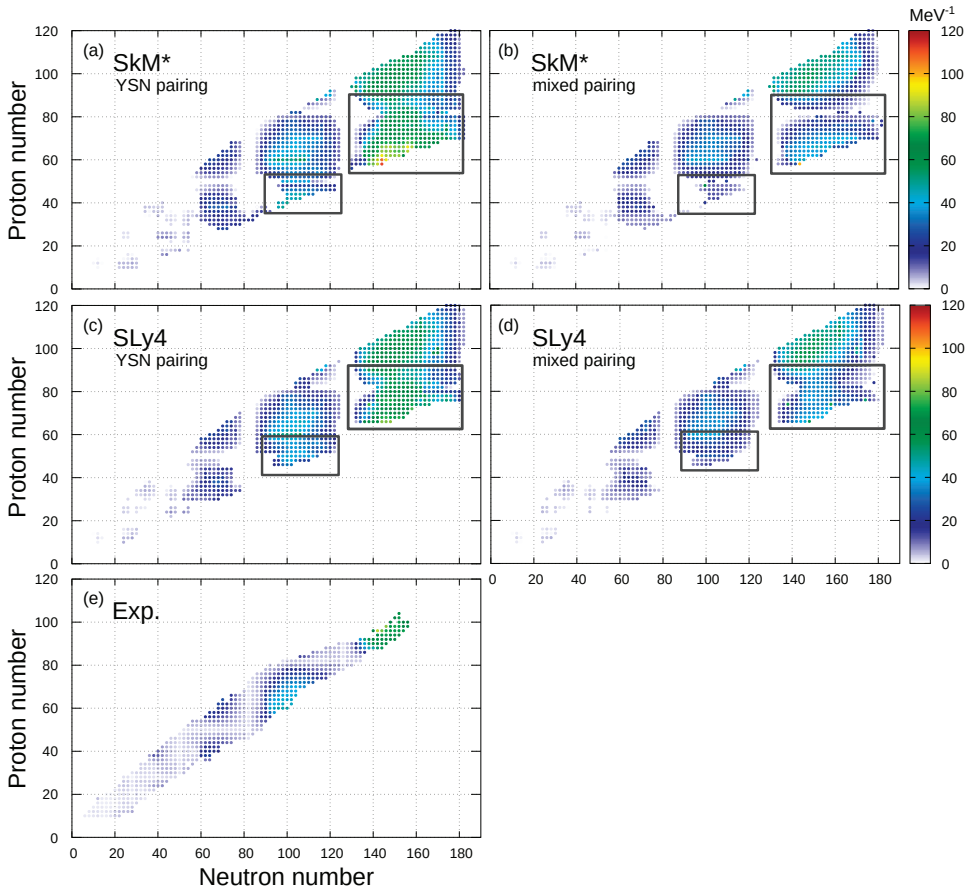

Fig. 1. – Calculated moments of inertia $\mathcal{J}$ for the SkM* and SLy4 functionals. The experimental data are taken from ref. [37], which is evaluated as $3/E(2_1^+)$.

Furthermore, one sees a distinct deviation from the straight line for the highest region around $\mathcal{J} = 60$ MeV^{-1}: ^{238,240}Cm and ^{244}Cf.

To make a quantitative measure of the theoretical accuracy, I compare theory and experiment, and examine the statistical properties of the quantity $R = \mathcal{J}_{\rm th}/\mathcal{J}_{\rm exp}$. Here $\mathcal{J}_{\rm th}$ and $\mathcal{J}_{\rm exp}$ are the theoretical and experimental MoI. A histogram of the distribution of R is shown in figs. 2(c) and 2(d). For SkM* (SLy4), the average is $\bar{R} = 1.02$ (1.16). When excluding the weakly deformed nuclei with $\beta < 0.1$, $\bar{R} = 1.07$ (1.15) for 332 (350) data. Therefore, the present model overestimates the MoI by about 10%.

The width of the distribution is an important quantity to determine the accuracy and reliability of the theory. One sees that the error is systematic, and the overall distribution is strongly peaked when excluding the weakly deformed nuclei that cause a tail in small R. The root-mean-square deviation, the dispersion, of R about its mean is $\sigma = 0.30$ (0.35).

It is interesting to compare the present calculation with the beyond-mean-field type calculations [38, 39]. The excited 2^+ states were obtained by the minimization after projection (MAP) and the generator coordinate method (GCM) using the SLy4 func-

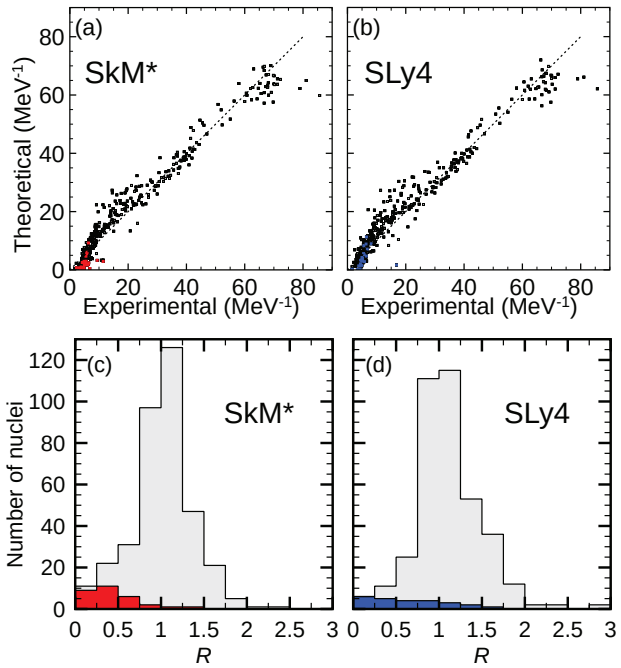

Fig. 2. – Calculated MoI for 362 nuclei for the SkM* functional (a) and 375 nuclei for the SLy4 functional (b) augmented by the YSN pairing functional are plotted *versus* experimental ones. Filled symbols indicate 30 (25) nuclei possessing a weak deformation with $\beta < 0.1$ with SkM* (SLy4). Histogram of the quantity $R = \mathcal{J}_{\rm th}/\mathcal{J}_{\rm exp}$ for the SkM* (c) and SLy4 (d) data set. The area in the dark indicates nuclei possessing a weak deformation with $\beta < 0.1$.

tional [38] or the 5-dimensional collective Hamiltonian (5DCH) based on the GCM together with the Gaussian overlap approximation using the Gogny D1S functional [39]. The authors in refs. [38,39] introduced the measure $R_E = \ln(E_{\rm th}(2^+)/E_{\rm exp}(2^+))$ to evaluate the validity of the theoretical framework. Then, I evaluate $E(2^+)$ as $3/\mathcal{J}$ in the present model.

Table I summarizes the statistics for the performance. The present model gives a compatible description for the average of the energy to the 5DCH approach for deformed nuclei. The dispersion is also comparable to these models. This comparison indicates that the 2_1^+ state is mostly governed by the rotational MoI of the ground state, and the self-consistent cranking model describes the 2_1^+ state surprisingly well for deformed nuclei with $\beta > 0.1$. However, it does not mean the rotational band with the excitation energy $\propto I(I+1)$ appears even above $I = 2$ because I have evaluated the MoI in the limit of $\omega_{\rm rot} = 0$.

I briefly mention the performance of the intrinsic quadrupole deformation. For selected nuclei of the Nd and Sm isotopes, it was demonstrated that the mean-field approximation describes well the evolution of deformation; see fig. 1 of ref. [40]. There are 396 even-even nuclei with known β [37], where the deformation parameter is evaluated from the $E2$ transition probability: $\beta = (4\pi/3ZR_0^2)\sqrt{B(E2)/e^2}$ [2]. I exclude 10 very light nuclei ($Z < 10$). Additional 156 (146) spherical nuclei have been eliminated as in the above analysis, leaving 230 (240) nuclei. I define the measure $R_\beta = \ln(\beta_{\rm cal}/\beta_{\rm exp})$

TABLE I. – *Statistics for the performance of the CHFB calculations. Averages $\bar{R}_E$ and standard deviations σ_E for measured $E(2^+)$ are summarized. The values for MAP and GCM are taken from ref.* [38]*, while 5DCH is from ref.* [39]*. The mixed and surface-type pairings correspond to the EDF with $\eta_0 = 0.5, \eta_1 = \eta_2 = 0$ and $\eta_0 = 1, \eta_1 = \eta_2 = 0$ in Eq. (3), respectively.*

model	# of nuclei	$\bar{R}_E$	σ_E
CHFB (SkM*+YSN)	332	−0.021	0.33
CHFB (SkM*+mixed)	325	0.029	0.35
CHFB (SLy4+YSN)	350	−0.095	0.30
CHFB (SLy4+mixed)	356	−0.053	0.37
MAP (SLy4+surface)	359	0.28	0.49
MAP (SLy4+surface)	135 (deformed)	0.20	0.30
GCM (SLy4+surface)	359	0.51	0.38
GCM (SLy4+surface)	135 (deformed)	0.27	0.33
5DCH (D1S)	519	0.12	0.33
5DCH (D1S)	146 (deformed)	−0.05	0.19

similarly to $E(2_1^+)$. I then find $\bar{R}_\beta = -0.12(-0.11)$ with the dispersion $\sigma = 0.35(0.30)$ for SkM* (SLy4), and $\bar{R}_\beta = -0.08(-0.09)$, $\sigma = 0.26(0.22)$ for 219 (233) nuclei with $\beta > 0.1$. The performance is as good as for the MoI.

3˙2. *MoI of neutron-rich nuclei.* – Then, I investigate the MoI of neutron-rich nuclei, and discuss unique features near the drip line. A striking feature observed in the result shown in fig. 1 is that the predicted MoI strongly depended on the pairing functional employed in the calculations, as indicated by squared regions. Figures 1(a) and 1(c) show the calculated MoI with the YSN pairing. I include the even-even nuclei up to $Z = 120$ and below the magic number of $N = 184$. The MoI of the rare-earth nuclei near the drip line are comparable to those of the heavy actinide nuclei, although the mass number is different by about 40. The calculated MoI obtained by employing a mixed-type pairing EDF do not show such an enhancement near the drip line, as shown in figs. 1(b) and 1(d).

A significant enhancement of MoI near the drip line using the YSN functional is due to a deformed-shell effect and an isovector-density dependence (an effective decrease in the strength) of the pairing functional. Indeed, this mechanism explains the lowering of $E(2_1^+)$ in ^{40}Mg [28]. The reduction in the strength of the pair interaction with an increase in the asymmetry can be seen by the comparison of figs. 3(a) and 3(b). A reduction of the MoI relative to the rigid body is due to the pairing, and the reduction found in very neutron-rich nuclei with the asymmetry $\alpha = (N - Z)/A > 0.3$ is apparently weakened when using the YSN pairing functional. Scattering of the data points is associated with the shell effect.

As the quadrupole collectivity increases, one sees a lower energy and a stronger transition. Empirically, the following relation has been found and 91% of the observed 328 data points are reproduced within a factor of two [41]:

$$\left[\frac{B(E2; 0_1^+ \to 2_1^+)}{1\, e^2\mathrm{fm}^4}\right] \times \left[\frac{E(2_1^+)}{1\,\mathrm{MeV}}\right] = 32.6\frac{Z^2}{A^{0.69}}. \tag{4}$$

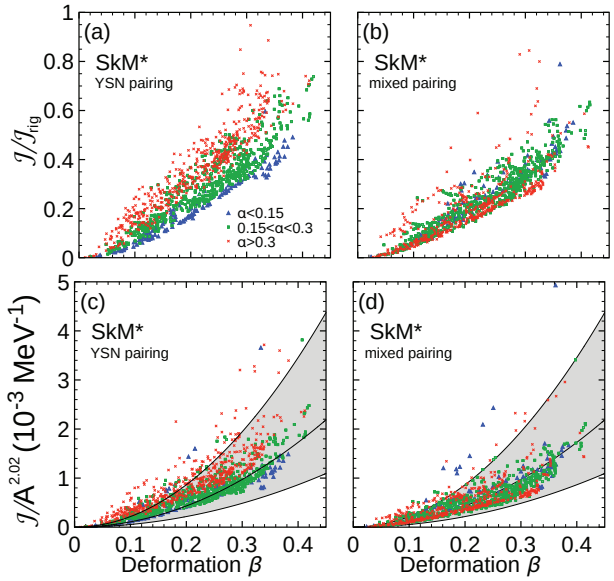

Fig. 3. – The ratio of the MoI calculated by using the YSN (a) and mixed-type (b) pairing functional and the ones for the rigid body. The calculated MoI divided by $A^{2.02}$ as a function of the deformation parameter β using the YSN (c) and mixed-type (d) pairing. The line represents Eq. (5) with the approximation $R_0 = 1.2A^{1/3}$ fm, and the uncertainty (a factor of two) is indicated by the shaded area. Symbols of triangle, square, and cross indicate the asymmetry parameter $\alpha < 0.15$, $0.15 \leq \alpha < 0.3$, and $\alpha \geq 0.3$, respectively.

This corresponds to

$$\mathcal{J} = \frac{3}{32.6}\left(\frac{3}{4\pi}\right)^2 A^{0.69} R_0^4 \beta^2 \ \ [\mathrm{MeV}^{-1}], \tag{5}$$

where R_0 is given in the unit of fm. Figures 3(c) and 3(d) show the calculated MoI divided by $A^{2.02}$ as a function of the deformation parameter β. With the mixed-type pairing, the calculated MoI scatter around the empirical line, and most of them are within a factor of two. On the other hand, with the YSN functional, the empirical line is entirely off the trend of the calculated MoI for $\alpha > 0.3$. Therefore, $E(2_1^+)$ can be low in neutron-rich nuclei despite the $B(E2)$ value is not high. A systematic measurement of $E(2_1^+)$ and $B(E2)$ in neutron-rich nuclei deepens the understanding of the pairing in nuclei and puts a constraint on the pairing density functional.

4. – Summary

I have performed systematic calculations of the MoI from the proton drip line to the neutron drip line to see the roles of neutron excess in the collective rotational motion. To describe neutron-rich nuclei where loosely bound neutrons and the continuum coupling are necessary to consider, the cranked HFB equation is solved in the coordinate space. The comparison with the available experimental data and other models shows that the present model surprisingly well describes the ground-state MoI, namely the $E(2_1^+)$ value, for deformed nuclei with $\beta > 0.1$. By employing the pairing density functional constructed to describe the isospin dependence in neutron-rich nuclei, I have found that the MoI can be greatly enhanced near the drip line, whereas the magnitude of deformation

is not as strong as estimated by the empirical relation between the $E(2_1^+)$ and $B(E2)$ values. A systematic measurement of $E(2_1^+)$ and $B(E2)$ in neutron-rich nuclei puts a constraint on the density dependence of the pairing effective interaction.

REFERENCES

[1] Hess G. B. and Fairbank W. M., *Phys. Rev. Lett.*, **19** (1967) 216.
[2] Ring P. and Schuck P., *The nuclear many-body problem* (Springer-Verlag, New York) 1980.
[3] Brink D. M. and Broglia R. A., *Nuclear Superfluidity: Pairing in Finite Systems*, *Cambridge Monographs on Particle Physics, Nuclear Physics and Cosmology* (Cambridge University Press) 2005.
[4] *Shell Evolution And Search for Two-plus energies At RIBF: SEASTAR project*, `https://www.nishina.riken.jp/collaboration/SUNFLOWER/experiment/seastar/index.php`.
[5] Gade A., *Eur. Phys. J. A*, **51** (2015) 118.
[6] Otsuka T. *et al.*, *Rev. Mod. Phys.*, **92** (2020) 015002.
[7] Crawford H. L. *et al.*, *Phys. Rev. Lett.*, **122** (2019) 052501.
[8] Terasaki J. *et al.*, *Nucl. Phys. A*, **621** (1997) 706.
[9] Rodríguez-Guzmán R., Egido J. and Robledo L., *Nucl. Phys. A*, **709** (2002) 201.
[10] Yoshida K., *Eur. Phys. J. A*, **42** (2009) 583.
[11] Yoshida K., *Mod. Phys. Lett. A*, **25** (2010) 1783.
[12] Yao J. M. *et al.*, *Phys. Rev. C*, **83** (2011) 014308.
[13] Watanabe S. *et al.*, *Phys. Rev. C*, **89** (2014) 044610.
[14] Rodríguez T. R., *Eur. Phys. J. A*, **52** (2016) 190.
[15] Shimada M. *et al.*, *Phys. Rev. C*, **93** (2016) 064314.
[16] Dobaczewski J., Flocard H. and Treiner J., *Nucl. Phys. A*, **422** (1984) 103.
[17] Terán E., Oberacker V. E. and Umar A. S., *Phys. Rev. C*, **67** (2003) 064314.
[18] Blazkiewicz A. *et al.*, *Phys. Rev. C*, **71** (2005) 054321.
[19] Yoshida K. and Van Giai N., *Phys. Rev. C*, **78** (2008) 014305.
[20] Oba H. and Matsuo M., *Prog. Theor. Phys.*, **120** (2008) 143.
[21] Pei J. C. *et al.*, *Phys. Rev. C*, **78** (2008) 064306.
[22] Kasuya H. and Yoshida K., *Prog. Theor. Exp. Phys.*, **2021** (2021) 013D01.
[23] Terasaki J. *et al.*, *Nucl. Phys. A*, **600** (1996) 371.
[24] Jin S., Bulgac A., Roche K. and Wlazłowski G., *Phys. Rev. C*, **95** (2017) 044302.
[25] Kashiwaba Y. and Nakatsukasa T., *Phys. Rev. C*, **101** (2020) 045804.
[26] Bonche P., Flocard H. and Heenen P., *Nucl. Phys. A*, **467** (1987) 115.
[27] Ogasawara H. *et al.*, *Prog. Theor. Phys.*, **121** (2009) 357.
[28] Yoshida K., *Phys. Rev. C*, **105** (2022) 024313.
[29] *ScaLAPACK—Scalable Linear Algebra PACKage*, `http://www.netlib.org/scalapack/`.
[30] Baran A. *et al.*, *Phys. Rev. C*, **78** (2008) 014318.
[31] Yoshida K., *Phys. Lett. B*, **834** (2022) 137458.
[32] Bartel J. *et al.*, *Nucl. Phys. A*, **386** (1982) 79.
[33] Chabanat E. *et al.*, *Nucl. Phys. A*, **635** (1998) 231; *Nucl. Phys. A*, **643** (1998) 441(E).
[34] Yamagami M., Shimizu Y. R. and Nakatsukasa T., *Phys. Rev. C*, **80** (2009) 064301.
[35] Margueron J., Sagawa H. and Hagino K., *Phys. Rev. C*, **76** (2007) 064316.
[36] Margueron J., Sagawa H. and Hagino K., *Phys. Rev. C*, **77** (2008) 054309.
[37] *National Nuclear Data Center, "Evaluated Nuclear Structure Data File"*, `https://www.nndc.bnl.gov/ensdf/`.
[38] Sabbey B. *et al.*, *Phys. Rev. C*, **75** (2007) 044305.
[39] Bertsch G. F. *et al.*, *Phys. Rev. Lett.*, **99** (2007) 032502.
[40] Yoshida K. and Nakatsukasa T., *Phys. Rev. C*, **83** (2011) 021304.
[41] Raman S., Nestor C. and Tikkanen P., *At. Data Nucl. Data Tables*, **78** (2001) 1.